

## ATOM POSITIONS IN HIGHLY ORDERED KAOLINITE

P. R. SUITCH AND R. A. YOUNG

School of Physics, Georgia Institute of Technology, Atlanta, Georgia 30332

**Abstract**—The crystal structure of kaolinite ( $P1$ ,  $a = 5.153(1)$ ,  $b = 8.941(1)$ ,  $c = 7.403(1)$  Å,  $\alpha = 91.692(3)^\circ$ ,  $\beta = 104.860(3)^\circ$ ,  $\gamma = 89.822(3)^\circ$ , specimens from Keokuk geodes) has been refined in detail and that of dickite ( $Cc$ ,  $a = 5.1460(3)$ ,  $b = 8.9376(5)$ ,  $c = 14.4244(6)$  Å,  $\beta = 96.761(5)^\circ$ ) has been re-refined, both from powder diffraction data with the Rietveld method. Except for the hydrogen atoms, the layer structures in both clays are very similar and are much as inferred or determined previously by others. The rotation in the tetrahedral sheet is  $7(1)^\circ$ . The two inner hydroxyl O–H bonds in kaolinite are differently oriented; one points into an octahedral vacancy and the other somewhat away from the octahedral sheet and toward the unoccupied center of an oxygen triangle formed by the two apical oxygens and shared basal oxygen of two adjacent  $\text{SiO}_4$  tetrahedra. All six of the inner surface hydrogen atoms appear to be nearly equally involved in the hydrogen bonding between kaolinite layers in kaolinite.

**Key Words**—Crystal structure, Dickite, Hydrogen atom, Hydroxyl orientation, Kaolinite, Rietveld method.

### INTRODUCTION

Kaolinite, dickite, and nacrite are based on essentially the same structural element, a layer of composition  $\text{Al}_2\text{Si}_2\text{O}_5(\text{OH})_4$ . Each of these basic layers can be regarded as consisting of a tetrahedral sheet of  $\text{SiO}_4$  tetrahedra and an octahedral sheet of Al octahedrally coordinated by O and OH. Alternatively, one may think of the layer as being composed of five planes of atoms stacked together and consisting of, successively, O, Si, (O, OH), Al, and OH (e.g., Norton, 1973). The actual positions of the non-hydrogen atoms in kaolinite were deduced rather closely by Brindley and Robinson (1946), who also determined that the actual crystal lattice was triclinic with probable space group  $P1$ . Later, Brindley and Nakahira (1958) deduced that some distortions exist in the octahedral sheet and that the  $\text{SiO}_4$  tetrahedra are rotated about  $10^\circ$  from their earlier assigned symmetric positions. From an electron diffraction structure study (excluding H atoms), Zvyagin (1960) inferred that the silicate tetrahedra are rotated about  $20^\circ$  from Brindley and Robinson's symmetrical positions. Positions thought to be probable for the H atoms were reported by Giese and Datta (1973) on the basis of energy calculations, previous infrared studies, and the Zvyagin (1960) model.

The structure of dickite, except for the hydrogen atoms, was refined by Newnham and Brindley (1956, 1957) and was further refined by Newnham (1961) from single-crystal X-ray diffraction data. Newnham's 1956 results were used by Brindley and Nakahira (1958) to improve the structural model of the kaolinite layer. The similarity of dickite and kaolinite has been further emphasized by Bailey (1963) who demonstrated that an equally valid and mineralogically preferred choice of unit cell for dickite leads to  $\beta = 103.58^\circ$ , almost identical to that for kaolinite, rather than the  $\beta = 96.73^\circ$

value arising from Newnham's (1961) choice of cell. Kaolinite and dickite, however, do have some marked differences: (1) no kaolinite single crystals of size usable for X-ray diffraction structure studies are known; (2) layer stacking disorder (nb/3 shifts) is all but ubiquitous in kaolinite from all sources, whereas dickite rarely exhibits such disorder (Brindley and Porter, 1978); and (3) thirteen non-H atoms are present in the asymmetric unit of dickite, and four of these units combine according to space group  $Cc$  to make up the unit cell. The asymmetric unit of kaolinite (which is the entire unit cell, space group  $P1$ ) contains 26 non-H atoms in two pseudo-equivalent sets of 13, each similar to the 13 non-H atoms in dickite. Considering the near identity of the "kaolinite layer" in dickite to that in kaolinite, the questions arise as to just how nearly identical are they in detail and how can the differences in crystallization and disorder be explained? The present work presents a detailed structure refinement of kaolinite and a re-refinement of the structure of dickite using the Rietveld method to answer these questions.

### MATERIALS AND METHODS

Kaolinite from geodes found near Keokuk, Iowa, was kindly provided by Dr. W. D. Keller. Kaolinite from this general locality (Hayes, 1963; Keller *et al.*, 1966) is remarkable in that much of it is essentially free of the nb/3 shifting that is characteristic of kaolinite from other sources. The lack of nb/3 shifting was crucial to the success of this study because including its effects in the structure refinement would be a non-trivial task and has not been done. Two samples showing the least nb/3 shifting were selected, and the  $<37\text{-}\mu\text{m}$  particle size fractions were used as the study specimens (K27A and K31A).

Dickite from Ouray, Colorado, obtained from Wards

Natural Science Establishment, Rochester, New York (H-14), was also examined.

X-ray powder diffraction data were collected with crystal-monochromated  $\text{CuK}\alpha$  radiation ( $\lambda = 1.5405$  and  $1.5443 \text{ \AA}$ ) and a diffractometer operating in the step-scan mode at  $100 \text{ sec}/0.0375^\circ 2\theta$  step ( $0.05^\circ$  for dickite) over the  $2\theta$  range  $10^\circ$ – $104^\circ$ . Neutron powder diffraction data were collected from specimen K31A at Brookhaven National Laboratory by the courtesy and with the assistance of D. E. Cox. Because of the large incoherent scattering of thermal neutrons by hydrogen, a “third axis” was used to eliminate most of the inelastic portion of it. Most of the incoherent scattering is elastic, however, and it so degraded the signal-to-noise ratio that two full days of operation were required to produce a usable pattern over the  $2\theta$  range  $17^\circ$ – $126^\circ$  with  $\lambda = 2.3850 \text{ \AA}$ .

The structure refinements were carried out from both X-ray and neutron powder diffraction data with the Rietveld method (Rietveld, 1969; Young and Wiles, 1981). Version DBW 3.2 of a locally written computer program (Wiles and Young, 1981) was used with a pseudo-Voigt profile function.

Lattice parameters were refined simultaneously with the atomic parameters and other needed parameters (e.g., zero point, reflection profile breadth, background, asymmetry, preferred orientation) and an overall temperature factor. Test refinements with individual isotropic temperature factors, fixed in both kaolinite and dickite at the values given by Newnham (1961) showed that the positional parameters were not affected by using only an overall temperature factor instead of the fixed individual isotropic temperature factors. For most of the refinements with X-ray data, only the range  $10^\circ \leq 2\theta \leq 81^\circ$  was used because (1) the very large number of Bragg reflections tended to produce some computational difficulties, and (2) the severe multiple overlapping of reflections in the higher region tended to diminish the amount of extractable information. Test refinements with the atom site occupancies that were varied simultaneously with the other parameters did not indicate any significant departure from stoichiometry. The site occupancies were henceforth fixed at unity; however, the data used in these refinements do not extend effectively over a  $(\sin \theta)/\lambda$  range large enough to support simultaneous refinement of thermal factors and site occupancies nor to provide precision better than  $\sim 10\%$  when only site occupancies were refined with the thermal parameters kept fixed.

The dickite structure (except for H atoms) was refined from X-ray powder diffraction data primarily to assure that the refinement procedures were working properly, as judged by the agreement of our results with pre-existing single crystal results of Newnham (1961).

The non-H portion of the kaolinite structure was then refined for both specimens K27A and K31A: (1) starting from the Brindley and Robinson (1946) co-

ordinates (BRO model), and (2) starting from Zvyagin's (1960) coordinates (ZO model). In each refinement, the starting positions for the second set of 13 atoms were generated by application of  $\frac{1}{2}a + \frac{1}{2}b$  to the coordinates given by the cited authors for the first set of 13. Because the actual kaolinite atom positions in space group  $P1$  are close to those demanded for C-face centering, this procedure produced usable starting parameters for all 26 non-H atoms. The purposes in working with the two starting models were to test each directly for correctness and to assure that the same refined model would result from different starting parameters, i.e., that there were no false minima in the neighborhood. The refinements made with the X-ray data included tests for O(H) disorder about the average plane of the OH sheet (no positive result). The H and associated O(H) positions were then refined from the neutron data (K31A only). For the refinements with neutron data, all atoms other than H and O(H) were fixed at the positions determined from the X-ray data. Again, two different starting models were used: (1) model GDO was based on the H positions postulated by Giese and Datta (1973), and (2) model AHO was based on the H positions determined in dickite by Adams and Hewat (1981) from Rietveld refinements with neutron powder diffraction data. As with the X-ray refinements, the atom positions in the second half cell of the starting models were generated from those in the first half by C-face centering.

The principal criteria for the success of the Rietveld refinements were R values, the appearance of pattern-fitting plots (e.g., Figure 1) and, as in any crystal structure refinement, stereochemical reasonableness of the refined structure. The two types of R values most considered were  $R_{wp}$  (“R weighted pattern”) and  $R_B$  (“R Bragg”), as follows:

$$R_{wp} = \left[ \sum_i w_i (y_i(o) - y_i(c))^2 / \sum_i w_i (y_i(o))^2 \right]^{1/2} \quad \text{and} \quad (1)$$

$$R_B = \frac{\sum_H |I_H(\text{“o”}) - I_H(c)|}{\sum_H I_H(\text{“o”})}, \quad (2)$$

where  $y_i$  is the intensity at the  $i^{\text{th}}$  step in the pattern, o and c indicate observed and calculated, respectively,  $w_i$  is the weight, H signifies the Miller indices  $h, k,$  and  $l$ ,  $I_H$  is the intensity of Bragg reflection H, and “o” means that the intensity  $I(\text{“o”})$  was not observed independently for overlapped reflections but was the portion of the total overlapped intensities allocated to the  $H^{\text{th}}$  reflection on the basis of calculated intensity ratios. A discussion of the role of each of these fitting criteria has been given by Young and Wiles (1981).

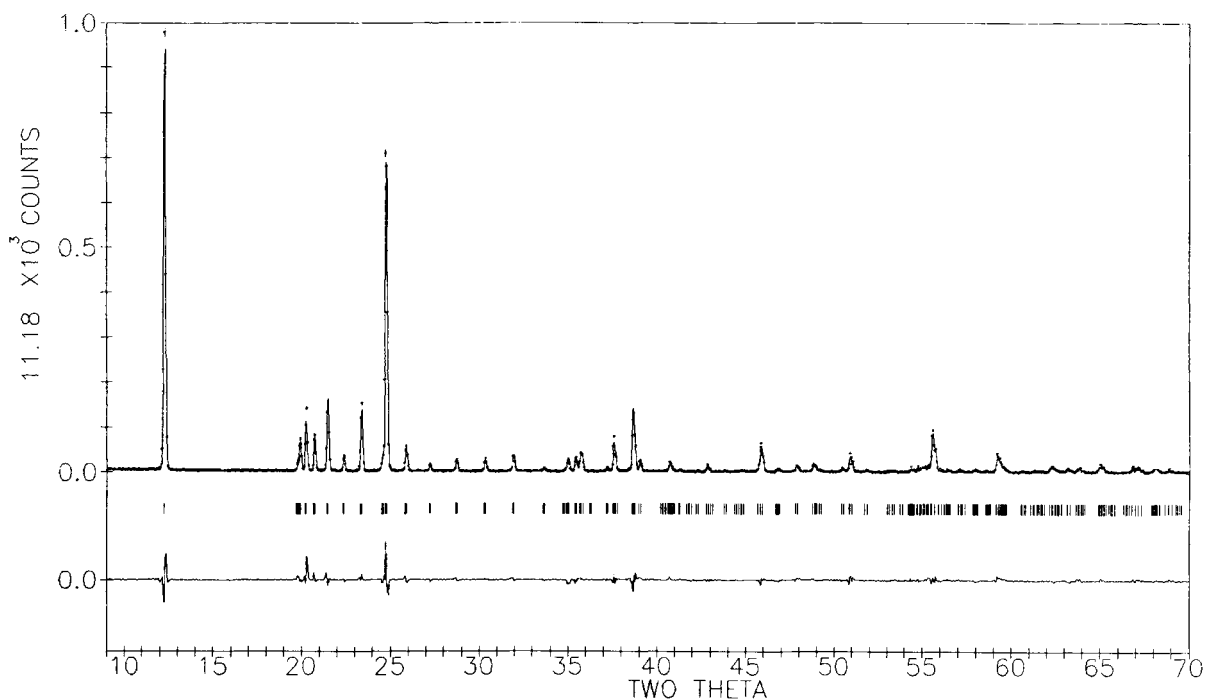


Figure 1. Pattern-fitting plot for Rietveld refinement of the dickite structure with X-ray diffraction data. In the upper field, the observed data are shown as dots with vertical error bars through them, and the calculated pattern is shown as the solid curve. The difference (observed minus calculated) is shown in the lower field. The short vertical bars in the middle field mark the positions of possible Bragg reflections.

## RESULTS

### *Test of procedure with dickite*

The results for the refinements of the dickite structure from X-ray powder diffraction data are shown in Table 1 and Figure 1. Using Newnham's (1961) estimated precision of 0.02 Å as the standard deviation, only 2 structural parameters ( $y$  of OH(1) and  $x$  of O(H7)) differ by as much as  $4\sigma$  (combined) between his results and ours and 3 which differ by about  $3\sigma$  ( $z$  of O(6),  $x$  of O(9), and  $y$  of Si(3)). Thus, the present Rietveld structure refinement results based on powder data are in good agreement with Newnham's single crystal results within the limits to be expected on the basis of the combined estimated standard deviations obtained from those calculated in the Rietveld procedure procedure and those estimated by Newnham (1961). It was therefore concluded that the Rietveld structure refinement procedure was appropriate for this problem.

### *Kaolinite structural results and tests for model and specimen dependence*

With two exceptions, lattice parameters and a possible pattern in O(H)  $z$  parameter differences, the X-ray structural results obtained for the two kaolinites using the two starting models (BRO and ZO) did not differ significantly. Therefore, only the results for K31A are

presented in Table 2 and Figure 2. The lattice parameters obtained for K27A were  $a = 5.1543(2)$ ,  $b = 8.9423(4)$ ,  $c = 7.4032(3)$  Å, and  $\alpha = 91.706(3)$ ,  $\beta = 104.859(3)$ ,  $\gamma = 89.818(3)^\circ$ . These values differ at most by  $\sim 3\sigma$  (combined) from those of sample K31A (Table 2). The e.s.d.'s on the structural parameters were generally 10–20% larger for sample K27A than for sample K31A. It may be relevant that only a small amount of nb/3 shift was discernable in the X-ray powder diffraction pattern of sample K27A. No shifting was detectable in the pattern of sample K31A (Figure 2).

To compare ZR and BRR, and thus to see if both starting models had led to the same result, it was necessary to determine the optimum transformation between the cells. (Because the space group is  $P1$ , the selection of the cell origin is completely arbitrary.) Normal projections of the two structures, BRR and ZR, onto the  $a, b$  plane were plotted as shown in Figure 3. Transparencies of these plots were then rotated and translated as necessary to produce the best visual fit of the two structures. This procedure produced the empirical transformation rule:

$$\begin{aligned} x_{\text{BRR}} &= \bar{x}_{\text{ZR}} + 0.323; \\ y_{\text{BRR}} &= \bar{y}_{\text{ZR}} + 0.148; \\ z_{\text{BRR}} &= \bar{z}_{\text{ZR}} + 0.449. \end{aligned} \quad (3)$$

This transformation was applied to the ZR results which

Table 1. Crystal structural parameters for dickite.

	Atomic coordinates					
	This work			Newnham (1961)		
	x	y	z	x	y	z
Al(2)	0.407(9)	0.425(2)	0.238(2)	0.419	0.417	0.231
Al(3)	0.921(7)	0.257(2)	0.238(2)	0.915	0.253	0.232
Si(2)	0.477(7)	0.572(2)	0.043(2)	0.500	0.573	0.040
Si(3)	-0.015(8)	0.405(2)	0.044(2)	0.012	0.400	0.041
O(2)	0.484(7)	0.585(4)	0.156(2)	0.511	0.581	0.153
O(5)	0.234(9)	0.475(4)	0.002(3)	0.259	0.472	-0.006
O(6)	0.066(12)	0.380(3)	0.164(3)	0.080	0.388	0.152
O(8)	-0.051(8)	0.238(5)	0.001(2)	-0.045	0.237	-0.006
O(9)	0.731(9)	0.501(3)	0.013(3)	0.765	0.511	0.006
O(H1)	0.589(9)	0.301(4)	0.168(3)	0.582	0.276	0.157
O(H4)	0.746(12)	0.391(4)	0.308(3)	0.747	0.395	0.298
O(H6)	0.333	0.587(5)	0.296	0.333	0.583	0.296
O(H7)	0.203(9)	0.267(5)	0.304(2)	0.244	0.273	0.295
	Other data					
	a (Å)	b (Å)	c (Å)	$\beta$ (deg)	R <sub>wp</sub> (%)	R <sub>a</sub> (%)
This work	5.1460(3)	8.9376(5)	14.4244(6)	96.761(5)	18.05	4.37
Newnham	5.150(1)	8.940(1)	14.424(2)	96.73(2)		

Table 2. Positional parameters from X-ray diffraction data for kaolinite (BRR and ZRT) and for dickite expressed in the kaolinite cell (NRT).<sup>1</sup>

Atom	BRR			ZRT			NRT		
	x	y	z	x	y	z	x	y	z
Al(1)	0.367(12)	0.490(6)	0.443(7)	0.353(10)	0.500(6)	0.434(7)	0.335(7)	0.480(2)	0.443(2)
Al(2)	0.339(13)	0.824(6)	0.425(7)	0.352(11)	0.815(6)	0.449(7)	0.349(9)	0.812(2)	0.443(2)
Al(3)	0.846(15)	-0.006(8)	0.442(9)	0.862(11)	-0.016(6)	0.449(7)	0.835(7)	-0.020(2)	0.443(2)
Al(4)	0.847(14)	0.314(7)	0.457(7)	0.834(11)	0.322(6)	0.431(7)	0.849(9)	0.312(2)	0.443(2)
Si(1)	0.047(12)	0.322(6)	0.070(7)	0.043(10)	0.309(6)	0.045(7)	0.066(8)	0.332(2)	0.055(2)
Si(2)	0.061(12)	0.662(6)	0.054(7)	0.073(10)	0.656(7)	0.059(10)	0.071(7)	0.665(2)	0.053(2)
Si(3)	0.544(14)	0.831(7)	0.048(7)	0.546(11)	0.822(6)	0.070(6)	0.566(8)	0.832(2)	0.055(2)
Si(4)	0.579(14)	0.156(7)	0.064(8)	0.569(12)	0.161(5)	0.057(7)	0.571(7)	0.165(2)	0.053(2)
O(1)	0.110	0.342	0.307	0.105(14)	0.340(9)	0.290(10)	0.114(12)	0.357(3)	0.295(3)
O(2)	0.170(17)	0.652(8)	0.278(10)	0.169(13)	0.667(7)	0.286(8)	0.181(7)	0.652(4)	0.279(2)
O(3)	0.039(15)	0.474(8)	-0.028(8)	0.067(16)	0.505(9)	-0.030(11)	0.053(8)	0.499(5)	-0.031(2)
O(4)	0.267(16)	0.228(7)	-0.011(8)	0.261(17)	0.212(8)	-0.004(9)	0.281(9)	0.236(3)	-0.007(3)
O(5)	0.252(16)	0.754(9)	-0.034(10)	0.244(16)	0.761(7)	-0.021(10)	0.270(9)	0.762(4)	-0.029(3)
O(6)	0.612(22)	0.836(11)	0.295(12)	0.616(14)	0.836(8)	0.294(9)	0.614(12)	0.857(3)	0.295(3)
O(7)	0.679(13)	0.167(8)	0.279(9)	0.677(15)	0.152(7)	0.279(8)	0.681(7)	0.152(4)	0.279(2)
O(8)	0.563(15)	0.004(8)	-0.026(9)	0.532	-0.029	-0.026	0.553(8)	-0.001(5)	-0.031(2)
O(9)	0.749(16)	0.714(7)	0.000(9)	0.758(17)	0.727(7)	-0.005(8)	0.781(9)	0.736(3)	-0.007(3)
O(10)	0.751(16)	0.263(8)	-0.020(9)	0.754(17)	0.253(8)	-0.036(9)	0.770(9)	0.262(4)	-0.029(3)
O(H1)	0.127(16)	-0.039(8)	0.307(9)	0.100(14)	-0.031(7)	0.273(9)	0.079(9)	-0.064(4)	0.303(3)
O(H2)	0.022(16)	0.158(9)	0.582(9)	0.012(16)	0.162(8)	0.554(8)	-0.009	0.150(5)	0.569
O(H3)	0.095(18)	0.462(9)	0.585(9)	0.108(12)	0.465(8)	0.571(9)	0.124(9)	0.470(5)	0.575(2)
O(H4)	0.101(14)	0.841(8)	0.590(8)	0.094(14)	0.851(6)	0.553(7)	0.071(12)	0.846(4)	0.583(3)
O(H5)	0.608(13)	0.468(8)	0.270(8)	0.640(12)	0.460(7)	0.303(9)	0.579(9)	0.436(4)	0.303(3)
O(H6)	0.513(17)	0.664(9)	0.558(9)	0.523(13)	0.660(8)	0.582(8)	0.491	0.650(5)	0.569
O(H7)	0.597(13)	-0.033(8)	0.570(8)	0.581(14)	-0.036(7)	0.583(10)	0.624(9)	-0.030(5)	0.575(2)
O(H8)	0.577(16)	0.351(9)	0.557(9)	0.586(15)	0.340(8)	0.590(9)	0.571(12)	0.346(4)	0.583(3)
	Other results from X-ray data								
	a (Å)	b (Å)	c (Å)	$\alpha$ (deg)	$\beta$ (deg)	$\gamma$ (deg)	R <sub>wp</sub> (%)	R <sub>B</sub> (%)	R <sub>exp</sub> (%)
BRR	5.1534(2)	8.9409(4)	7.4028(3)	91.692(3)	104.860(3)	89.821(3)	14.03	3.01	6.00
ZRT	5.1534(2)	8.9409(4)	7.4028(3)	91.692(3)	104.860(3)	89.822(3)	14.05	2.92	6.00

<sup>1</sup> BRR = Brindley and Robinson (1946); ZRT = Zvyagin (1960); NRT = Newnham (1961).

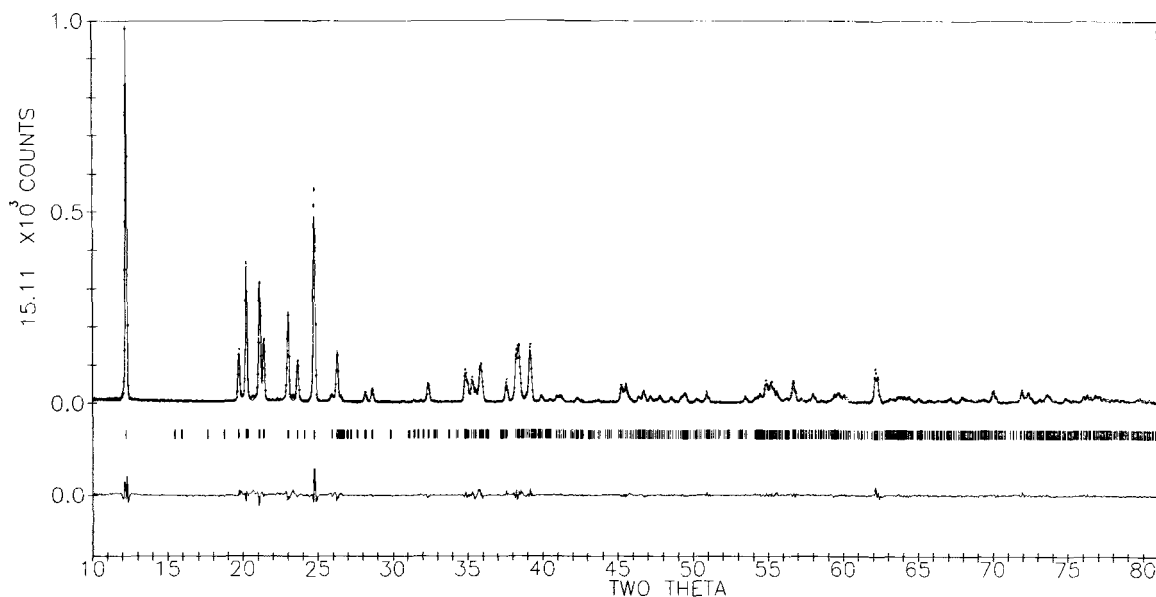


Figure 2. Pattern-fitting plot for Rietveld refinement of the structure of Keokuk kaolinite specimen K-31A with X-ray diffraction data, started from the Brindley and Robinson model (BRO) (see text). The format is as for Figure 1.

were obtained with the use of ZO as the starting model; the transformed results for sample K31A are given in Table 2 as ZRT. If the standard deviations in the individual parameters are considered, the ZR and BRR results are not significantly different. Only 2 of the 78 parameters differ by  $>3\sigma$  and 9 others by  $>2\sigma$ , much as could be expected for a normal distribution of errors. From such an atom by atom consideration it was concluded that the same refined structure was obtained no matter which set of starting parameters was used.

Further examination of the BRR results in Table 2 shows that, within the precision reported here, the non-H atom portions in kaolinite are consistent with the space group  $C1$ . However, the positions found for the inner hydroxyl H and the lattice parameters (especially the  $\alpha$  angle) confirm that the space group is, instead,  $P1$ .

#### Test for two-fold disorder in the O(H) sheet

Starting-model-dependent differences in the  $z$  coordinates of the inner surface hydroxyls are not readily apparent in individual groups of atoms. In both models, hydroxyl oxygen atoms (H 2, 3, 4, 6, 7, 8) were placed almost exactly on a plane, i.e., all 6 had almost the same  $z$  coordinates in each model. It can be seen from Table 2 that the O(H) atoms in the first half cell (H 2, 3, and 4) refined to positions "above" (larger  $z$ ) the starting plane, and those in the second half cell, to nominal positions below the starting plane for starting model BRO. For starting model ZO, just the opposite configuration is apparent (see ZRT in Table 2). The same result was obtained with sample K27A. These observations may be thought to suggest that the inner

surface O(H) atoms are actually in two-fold disorder about the average plane, as though their potential wells have double minima in  $z$ . Inasmuch as the separation of these hypothetical minima is only of the order of 2 or 3  $\sigma$ , such disorder cannot be confirmed with the present data. Further, the neutron-based AHR and GDR refinements do not show this same pattern.

#### Rotation of $SiO_4$ tetrahedra

The largest differences between the starting and final, refined models for the non-H atoms in kaolinite can be described as rotations of the  $SiO_4$  tetrahedra. These "rotations in the tetrahedral sheet" are primarily about

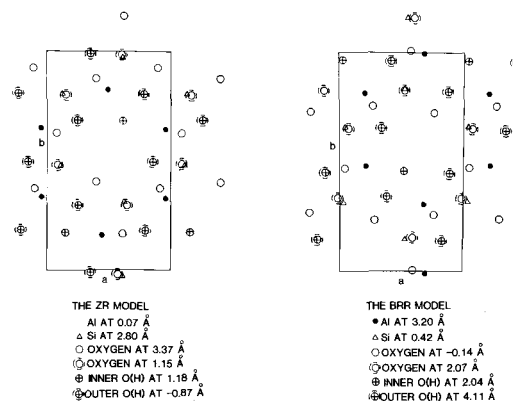


Figure 3. Comparison of the structure refined from the Brindley and Robinson model (BR) with that refined from the Zvyagin model (ZR). The projection is perpendicular to the  $a, b$  plane, and the numerical data are distances from it.

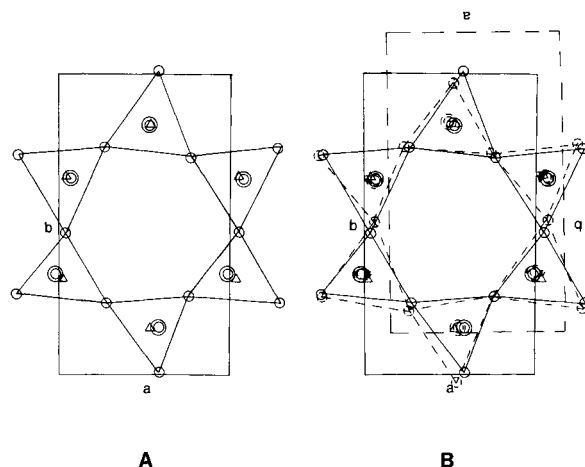


Figure 4. The tetrahedral sheets in the refined kaolinite structures projected onto the a,b plane. (a) In the BRR model,  $\Delta$  is Si,  $\odot$  is oxygen, and  $\circ$  is oxygen at 2.70, 1.09, and 3.23 Å, respectively, from the plane. (b) Superposition of the tetrahedral sheets in the BRR model (solid lines) and the ZR model (dashed lines) in visually judged best-fit positions. Note that, although the cell settings are different, the two models do describe the same final structure.

an axis perpendicular to the a,b plane, to which plane one face of each  $\text{SiO}_4$  tetrahedron is essentially parallel. (It is the oxygens on these faces that comprise the oxygen plane.) As a first approximation, Brindley and Robinson (1946) placed the tetrahedra rather symmetrically. Brindley and Nakahira (1958) suggested that a rotation of about  $10^\circ$  was probable. Zvyagin (1960) postulated a much larger rotation of  $20^\circ$ . The result with sample K31A is shown in Figure 4. The various tetrahedra are not obviously symmetric nor identically rotated. These imperfections, however, are mostly a matter of scatter of the representative atom-location points within a  $3\sigma$  range. From measurements of the angles between O face-edge lines in Figure 4 and from similar measurements for sample K27A, the average rotation of the tetrahedra is  $7(1)^\circ$ , substantially less than the value inferred by Zvyagin, but close to that inferred by Brindley and Nakahira ( $10^\circ$ ) and the same as that reported ( $8^\circ$ ) for dickite by Newnham and Brindley (1956). The importance of these rotations is attested to by Giese's (R. F. Giese, Jr., State University of New York at Buffalo, Amherst, New York, private communication, 1982) new energy-minimization cal-

Table 3. The O(H) and H positions in kaolinite (K-31A), Keokuk, Iowa.

	Refinement result AHR			Refinement result GDR		
	x	y	z	x	y	z
O(H1)	0.149(10)	0.191(6)	0.132(7)	0.199(12)	0.173(6)	0.131(7)
O(H2)	0.329(10)	-0.002(6)	-0.100(7)	0.327(14)	-0.007(6)	-0.110(8)
O(H3)	0.205(11)	0.691(6)	-0.133(9)	0.226(12)	0.677(6)	-0.125(8)
O(H4)	0.225(13)	0.296(6)	-0.124(8)	0.223(12)	0.301(6)	-0.112(7)
O(H5)	0.736(11)	0.679(5)	0.153(8)	0.669(10)	0.708(5)	0.146(8)
O(H6)	0.797(10)	0.502(6)	-0.133(8)	0.820(13)	0.507(6)	-0.105(8)
O(H7)	0.735(11)	0.171(6)	-0.114(8)	0.704(11)	0.186(6)	-0.113(8)
O(H8)	0.723(14)	0.814(7)	-0.133(9)	0.721(13)	0.806(6)	-0.145(8)
H(1)	0.070(17)	0.110(8)	0.087(10)	0.083(14)	0.106(7)	0.068(11)
H(2)	0.125(14)	-0.050(7)	-0.271(11)	0.168(13)	0.016(8)	-0.257(11)
H(3)	0.240(15)	0.640(10)	-0.235(12)	0.207(16)	0.636(9)	-0.279(1)
H(4)	0.255(15)	0.339(8)	-0.257(12)	0.278(14)	0.344(9)	-0.236(11)
H(5)	0.600(17)	0.585(8)	0.180(12)	0.617(16)	0.574(8)	0.179(11)
H(6)	0.712(15)	0.533(9)	-0.240(12)	0.620(12)	0.432(7)	-0.270(9)
H(7)	0.712(15)	0.142(9)	-0.285(11)	0.753(16)	0.149(10)	-0.254(13)
H(8)	0.745(19)	0.862(10)	-0.222(12)	0.728(14)	0.870(9)	-0.256(13)
	Starting model AHO			Starting model GDO		
	x	y	z	x	y	z
H(1)	0.127	0.083	0.207	0.133	0.094	0.120
H(2)	0.150	-0.008	-0.255	0.227	0.012	-0.271
H(3)	0.193	0.629	-0.263	0.273	0.669	-0.262
H(4)	0.209	0.356	-0.285	0.353	0.414	-0.159
H(5)	0.627	0.583	0.207	0.633	0.594	0.120
H(6)	0.650	0.492	-0.255	0.727	0.512	-0.271
H(7)	0.693	0.129	-0.263	0.773	0.169	-0.262
H(8)	0.709	0.856	-0.285	0.853	0.914	-0.159
	R values					
Refinement		$R_{wp}$	$R_{exp}$	$R_B$		
No.	Result	(%)	(%)	(%)		
RK171	AHR	5.50	5.26	1.02		
RK173	GDR	5.51	5.26	1.08		

Table 4. Interatomic distances (Å) and angles (°) for kaolinite.

O–O distances		Si–O distances		O(H)–H distances		
O(1)–O(2)	2.95(10)	Si(1)–O(1)	1.76(9)	O(H1)–H(1)	0.85(8)	0.88(8)
O(1)–O(3)	2.79(11)	Si(1)–O(3)	1.70(10)	O(H2)–H(2)	1.48(8)	1.21(9)
O(1)–O(4)	2.73(11)	Si(1)–O(4)	1.63(10)	O(H3)–H(3)	0.93(11)	1.17(10)
O(1)–O(7)	2.76(11)	Si(1)–O(10)	1.60(9)	O(H4)–H(4)	1.11(11)	1.10(11)
O(1)–O(10)	2.71(9)	Si(2)–O(2)	1.56(8)	O(H5)–H(5)	1.15(10)	1.27(8)
O(2)–O(1)	2.45(10)	Si(2)–O(3)	1.48(10)	O(H6)–H(6)	0.86(10)	1.52(8)
O(2)–O(3)	2.59(10)	Si(2)–O(5)	1.52(10)	O(H7)–H(7)	1.26(10)	1.17(12)
O(2)–O(5)	2.50(10)	Si(2)–O(9)	1.70(10)	O(H8)–H(8)	0.83(11)	1.02(11)
O(2)–O(6)	2.71(10)	Si(3)–O(5)	1.62(9)	H(outer)–O(next layer) distances		
O(2)–O(9)	2.65(9)	Si(3)–O(6)	1.71(8)	<u>AHR</u> <u>GDR</u>		
O(3)–O(1)	2.79(11)	Si(3)–O(8)	1.52(5)	H(2)–O(4)	1.99(10)	2.18(10)
O(3)–O(2)	2.59(10)	Si(3)–O(9)	1.61(10)	H(3)–O(3)	2.14(13)	1.88(12)
O(3)–O(5)	2.46(10)	Si(4)–O(4)	1.60(10)	H(4)–O(5)	2.05(11)	2.20(10)
O(3)–O(9)	2.56(11)	Si(4)–O(7)	1.60(8)	H(6)–O(9)	2.35(10)	1.95(9)
O(3)–O(10)	2.77(11)	Si(4)–O(8)	1.78(5)	H(7)–O(8)	1.96(9)	2.08(10)
O(4)–O(1)	2.73(11)	Si(4)–O(10)	1.56(10)	H(8)–O(10)	2.15(10)	1.90(11)
O(4)–O(3)	2.80(11)	O–Si–O angles		H(inner)–O(same layer) distances		
O(4)–O(7)	2.65(9)	O(1)–Si(1)–O(4)	107(4)	<u>AHR</u> <u>GDR</u>		
O(4)–O(8)	2.59(8)	O(1)–Si(1)–O(10)	108(5)	H(1)–O(4)apex	3.17(10)	3.30(11)
O(4)–O(10)	2.59(12)	O(1)–Si(1)–O(1)	108(5)	H(1)–O(7)apex	2.63(12)	2.75(11)
O(5)–O(6)	2.76(9)	O(3)–Si(1)–O(1)	108(5)	H(1)–O(1)apex	2.83(10)	2.80(10)
O(5)–O(8)	2.40(7)	O(3)–Si(1)–O(4)	114(5)	H(5)–O(6)apex	2.52(10)	2.41(10)
O(5)–O(9)	2.54(12)	O(3)–Si(1)–O(10)	114(5)	H(5)–O(2)apex	2.47(11)	2.52(11)
O(6)–O(7)	2.87(10)	O(4)–Si(1)–O(10)	106(5)	H(5)–O(9)basal	2.62(11)	2.59(11)
O(6)–O(8)	2.72(7)	O(3)–Si(2)–O(2)	117(5)	O(H(outer)–H . . . O (next layer) angles		
O(6)–O(9)	2.80(10)	O(3)–Si(2)–O(5)	110(6)	<u>AHR</u> <u>GDR</u>		
O(7)–O(8)	2.68(6)	O(5)–Si(2)–O(2)	109(5)	O(H2)–H(2) . . . O(4)	142(6)	141(6)
O(7)–O(10)	2.65(10)	O(9)–Si(2)–O(2)	109(5)	O(H3)–H(3) . . . O(3)	148(9)	157(7)
O(8)–O(9)	2.46(7)	O(9)–Si(2)–O(3)	107(5)	O(H4)–H(4) . . . O(5)	146(7)	138(6)
O(8)–O(10)	2.78(8)	O(9)–Si(2)–O(5)	104(5)	O(H6)–H(6) . . . O(9)	134(8)	136(6)
		O(5)–Si(3)–O(6)	103(3)	O(H7)–H(7) . . . O(8)	153(6)	156(7)
		O(5)–Si(3)–O(8)	100(3)	O(H8)–H(8) . . . O(10)	141(9)	143(7)
		O(8)–Si(3)–O(6)	115(4)	O–H angles with a,b plane		
		O(9)–Si(3)–O(5)	111(5)	<u>AHR</u> <u>GDR</u>		
		O(9)–Si(3)–O(8)	104(4)	O(H1)–H(1)	–23(7)	–31(7)
		O(9)–Si(3)–O(6)	115(4)	O(H2)–H(2)	56(5)	61(7)
		O(4)–Si(4)–O(7)	112(5)	O(H3)–H(3)	54(11)	77(13)
		O(4)–Si(4)–O(8)	100(4)	O(H4)–H(4)	61(12)	55(9)
		O(4)–Si(4)–O(10)	113(5)	O(H5)–H(5)	10(5)	11(5)
		O(8)–Si(4)–O(7)	105(3)	O(H6)–H(6)	65(15)	51(4)
		O(8)–Si(4)–O(10)	113(4)	O(H7)–H(7)	85(17)	62(12)
		O(10)–Si(4)–O(7)	114(5)	O(H8)–H(8)	52(12)	53(9)

The distances and angles not involving H are from the refinement result ZRT. Those involving H are from the refinement results AHR and GDR, as indicated (see text).

culations of the H positions. These results, based on a model with the silicate tetrahedra rotated as in Newham and Brindley (1956), are much closer to our results for the H positions than were the earlier values of Giese and Datta (1973) based on the Zvyagin (1960) model.

#### Hydrogen atoms

The 8 H and the 8 O(H) positions were refined from neutron data with the O, Si, and Al atoms fixed at their

ZR positions. The O(H)s were refined simultaneously with the Hs because the neutron-sensed and X-ray-sensed positions of the O(H) atoms may be expected to differ a little due to the H distortion of the electron cloud sensed by X-rays around the O(H) atoms. The pattern-fitting plot for the AHR refinement is shown in Figure 5. The pattern-fitting plot for the GDR refinement, resulting from the other starting model, is essentially indistinguishable and is therefore not shown.

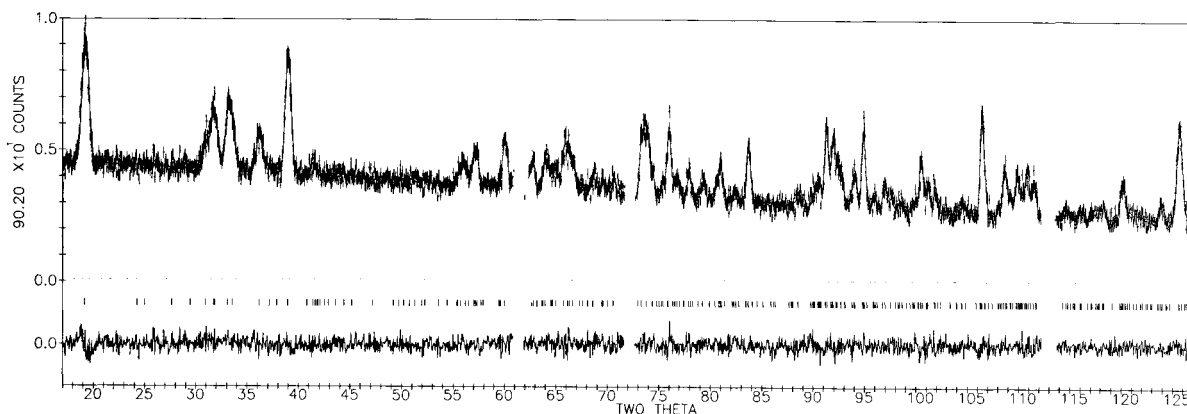


Figure 5. Pattern-fitting plot for Rietveld refinement of the H and O(H) positions with neutron data, starting with a model (AHO) based on the Adams and Hewat (1981) results for the H positions in dickite. The format is as for Figure 1.

Of the four H atoms in a half-cell, the three inner surface hydroxyl H atoms lie between the O(H) plane of one kaolinite layer and the O plane of the next one, 2.91 Å away. The fourth inner hydroxyl H is attached to an O(H) in the mixed O and O(H) plane. The H and O(H) coordinates for the two starting models and the two resulting refined models (GDR and AHR) are given in Table 3. The O–H . . . O bond angles and distances are given in Table 4 as calculated with ORFFE4 (Busing *et al.*, 1979).

As Table 4 shows, there is nothing stereochemically unusual in the O–H . . . O bond distances and angles for the H atoms which provide the hydrogen bonding that holds the layers together in kaolinite. Contrary to some previous reports (see Adams and Hewat (1981) for a discussion), all inner surface hydroxyl hydrogen atoms appear to be involved in the H bonding between layers in kaolinite; with the possible exception of H(6), all of the H–O hydrogen bond distances are within 2  $\sigma$  of 2.1 Å. The H(6)–O distance is only slightly greater, and that in only one of the two measures. Further, if the AHR and GDR O–H angle results are averaged, all 6 outer O–H directions make angles of between  $\sim 53(12)^\circ$  and  $73(15)^\circ$  with the plane of the O(H) atoms.

The most notable point of Table 4 is that the two inner hydroxyl H atoms differ decidedly in terms of how the O–H bond is directed. In the first half cell the O–H is directed into an octahedral vacancy with the hydrogen atom, H(1), being nearly equidistant from inner surface hydroxyl oxygen atoms O(H7) and O(H2) (2.05(9) and 2.36(10) Å in AHR and 2.20(8) and 2.26(11) in GDR, respectively). In the second half cell the O–H bond is directed somewhat away from the octahedral layer and toward the unoccupied center of an oxygen triangle formed by the two apical oxygens, O(6) and O(2), and the shared basal oxygen, O(9), of two adjacent SiO<sub>4</sub> tetrahedra. The O(H1)–H(1) distance (average of AHR and GDR) is 0.9(1) Å for the

O–H pointing into the octahedral vacancy and 1.2(1) Å for the O(H5)–H(5) bond pointing toward the unoccupied center of the oxygen triangle. The angles that these two O–H directions make with the plane of the mixed O and OH sheet (parallel to a,b) are about  $-27(10)^\circ$  and  $+11(7)^\circ$ , respectively. The difference in the inner O–H direction is the most obvious way in which the two halves of the kaolinite cell, otherwise nearly related by C-face centering, differ.

The two starting models appear to have led to different refined positions for H(2) and H(6), which are inner surface H atoms pseudorelated by C-face centering. In both refined models, H(2) bonds to O(4) in the next layer and H(6) to O(9), but the bond distances differ. The AHR vs. GDR results for H(2) differ by 2.3  $\sigma$  (combined) in x and 6.2  $\sigma$  in y. For H(6) they differ by 4.8  $\sigma$  in x and 8.9  $\sigma$  in y. To test both for false minima and two-fold disorder of H(2) and H(6) between two positions, a half-atom (of H) was placed at each position (AHR and GDR) for H(4) and H(6) and the site occupancies were refined. The site occupancies did not change from 0.5 by more than  $\sim 10\%$ , which is not much greater than  $\sigma$ . Thus, the possibility can not be ruled out that (1) the two apparent positions for H(2) and H(6) are not due to false minima, and (2) each of these atoms, H(2) and H(6), is statistically distributed equally (in two-fold disorder) between the two positions (AHR and GDR) apparently available to it.

#### Comparison of kaolinite and dickite

The refinement NR for dickite (Table 1 and Figure 1) was used to compare the non-H portions of the two clays because they were produced in the same way as the refinement results for kaolinite. To permit detailed comparison of the basic layer in kaolinite with that in dickite, the NR results were transformed to the BRR cell in Table 2 in the columns labeled NRT. (See Table 5 for the appropriate mapping procedure.) Except



Table 5. Labels used by various authors for the same atoms.

<i>In kaolinite</i>		
This work	Zvyagin (1960)	Newnham (1961)
Al(1)		
Al(2)	Al(2)	Al(2)
Al(3)	Al(1)	Al(1)
Al(4)		
O(1)		
O(2)		O(5)
O(3)		
O(4)	O(9)	
O(5)		O(2)
O(6)	O(4)	O(4)
O(7)	O(5)	
O(8)	O(8)	O(1)
O(9)		O(3)
O(10)	O(7)	
O(H1)	O6(H)	OH(1)
O(H2)	O2(H)	
O(H3)		
O(H4)	O3(H)	O(H3)
O(H5)		
O(H6)		O(H4)
O(H7)	O1(H)	O(H2)
OH(8)		
Si(1)		
Si(2)		Si(2)
Si(3)	Si(2)	Si(1)
Si(4)	Si(1)	

<i>In dickite</i>		
This work	Adams and Hewat (1981)	Giese and Datta (1976)
H(1)	H(1)	H(10)
H(2)	H(8)	H(8)
H(3)	H(6)	H(1)
H(4)	H(3)	H(9)
H(5)	H(5)	H(6)
H(6)	H(4)	H(2)
H(7)	H(2)	H(7)
H(8)	H(7)	H(3)

for the two inner hydroxyl oxygens, O(H1) and O(H5), the only difference  $> 3\sigma$  in the two layers are  $3.6\sigma$  in the y and  $3.9\sigma$  in the z of O(H5). Although some of these differences may be real, they are small and not dramatic. Even the rotations in the tetrahedral sheets are the same. This comparison of NRT data with BRR data tends to confirm the near identity of the non-H parts of the basic layers of dickite and kaolinite. Clearly, the inner hydroxyl orientations constitute a major difference between dickite, in which these two H atoms are crystallographically equivalent by a C-face centering translation, and kaolinite, in which they decidedly are not.

Because dickite does not exhibit nb/3 shifting as kaolinite does, despite the fact that the non-H parts of the basic layers are essentially the same in each, the interlayer hydrogen bonding may be stronger in dickite. If so, this should be reflected in shorter H–O interlayer bond distances. From the Adams and Hewat (1981) report, the average H–O distance (for inner surface

hydroxyl H atoms) is  $1.90(6)\text{ \AA}$ . That for the 6 H–O distances found for kaolinite in the present work is  $2.07(10)\text{ \AA}$  (averaged over both AHR and GDR results), which may be longer but is not statistically different. Likewise the average O–H . . . O angles, involving the inner surface H atoms, do not differ significantly between dickite and kaolinite ( $148(6)^\circ$  and  $144(7)^\circ$ , respectively). The calculated perpendicular distance allocated per kaolinite layer is  $0.0068(5)\text{ \AA}$  greater in dickite (based on the lattice parameters listed for the NRT data and BRR data in Table 1), which seems to be a statistically significant difference. It is possible, however, that systematic errors and real specimen to specimen differences may exist to produce lattice parameter differences which are this large.

### CONCLUSIONS

The principal differences between dickite and kaolinite that are determinable with present experimental precision are: (1) different orientations for the two inner O–H directions in kaolinite, which alone is enough to destroy the C-face centering found in dickite, and (2) possible allocation of slightly different perpendicular distances per kaolinite layer in the two clays, perhaps reflecting the different O to O(H) interactions between layers accompanying the c glide plane in dickite.

### ACKNOWLEDGMENTS

The authors are particularly grateful to Dr. W. D. Keller for first calling our attention to and then supplying the indispensable samples of Keokuk kaolinite and to Dr. D. E. Cox for contributing his time, skills, and limited neutron-diffractometer time. Appreciation is also expressed to Dr. W. E. Moody for his help in obtaining the specimens and for his interest and helpful discussions. This material is based in part upon work supported by the office of Surface Mining, Department of the Interior, under Grant G5105019 and continued by the Bureau of Mines under Grant G1115131.

### REFERENCES

- Adams, J. M. and Hewat, A. W. (1981) Hydrogen atom positions in dickite: *Clays & Clay Minerals* **29**, 316–319.
- Bailey, S. W. (1963) Polymorphism of the kaolin minerals: *Amer. Mineral.* **48**, 1196–1209.
- Brindley, G. W. and Nakahira, M. (1958) Further consideration of the crystal structure of kaolinite: *Min. Mag.* **31**, 781–786.
- Brindley, G. W. and Porter, A. R. D. (1978) Occurrence of dickite in Jamaica; ordered and disordered varieties: *Amer. Mineral.* **63**, 554–562.
- Brindley, G. W. and Robinson, K. (1946) The structure of kaolinite: *Min. Mag.* **27**, 242–253.
- Busing, W. R., Martin, K. O., Levy, H. A., Brown, G. M., Johnson, C. K., and Thiessen, W. E. (1979) *ORFFE4*. Accession No. 85, World list of crystallographic computer programs, 3rd ed., *J. Appl. Cryst.* **6**, 309–346.
- Giese, R. F., Jr. and Datta, P. (1973) Hydroxyl orientation in kaolinite, dickite, and nacrite: *Amer. Mineral.* **58**, 471–479.

- Hayes, J. B. (1963) Kaolinite from Warsaw geodes, Keokuk region, Iowa: *Iowa Acad. Sci.* **70**, 261–272.
- Keller, W. D., Pickett, E. E., and Reesman, A. L. (1966) Elevated dehydroxylation temperature of the Keokuk geode kaolinite—a possible reference mineral: *Proc. Inter. Clay Conf., 1966, Jerusalem, Israel, I*, L. Heller and A. Weiss, eds., Israel Prog. Sci. Transl., Jerusalem, 75–85.
- Newnham, R. E. (1961) A refinement of the dickite structure and some remarks on polymorphism in kaolin minerals: *Min. Mag.* **32**, 683–704.
- Newnham, R. E. and Brindley, G. W. (1956) The crystal structure of dickite: *Acta Crystallogr.* **9**, 759–764.
- Newnham, R. E. and Brindley, G. W. (1957) The structure of dickite: correction: *Acta Crystallogr.* **10**, p. 88.
- Norton, F. H. (1973) *Elements of Ceramics*: 2nd ed., Addison-Wesley, Reading, Massachusetts, p. 17.
- Rietveld, H. M. (1969) A profile refinement method for nuclear and magnetic structures: *J. Appl. Cryst.* **30**, 65–71.
- Wiles, D. B. and Young, R. A. (1981) New computer program for Rietveld analysis of X-ray powder diffraction patterns: *J. Appl. Cryst.* **14**, 149–151.
- Young, R. A. and Wiles, D. B. (1981) Application of the Rietveld method for structure refinement with powder diffraction data: *Adv. X-ray Anal.* **24**, 1–23.
- Zvyagin, B. B. (1960) Electron diffraction determination of the structure of kaolinite: *Kristallografiya* **5**, 32–41.

(Received 18 June 1982; accepted 30 March 1983)

**Резюме**—На основе данных рентгеновской порошковой дифракции, обработанных по методу Ретвельда, была подробно усовершенствована кристаллическая структура каолинита ( $P1$ ,  $a = 5,153(1)$ ,  $b = 8,941(1)$ ,  $c = 7,403(1)$  Å,  $\alpha = 91,692(3)^\circ$ ,  $\beta = 104,860(3)^\circ$ ,  $\gamma = 89,822(3)^\circ$ , образцы из кеокуовых жезд), а также более усовершенствована кристаллическая структура дикита ( $Cc$ ,  $a = 5,1460(3)$ ,  $b = 8,9376(5)$ ,  $c = 14,4244(6)$  Å,  $\beta = 96,761(5)^\circ$ ). Эа исключением атомов водорода, слоистые структуры обоих глин являются подобными и находятся в соответствии со структурами, ранее определенными другими исследователями. Вращение в тетраэдрическом слое составляет  $7(1)^\circ$ . Две внутренние связи O–H в каолините ориентированы по-разному; одна направлена в сторону октаэдрической пустоты, а другая направлена немного в сторону от октаэдрического слоя и по направлению к незанятому центру кислородного треугольника, образованного из двух апиальных атомов кислорода и одного основного атома кислорода, делииого между двумя прилегающими четырехгранниками  $SiO_4$ . Все шесть атомы водорода водорода внутренней поверхности, По-видимому, почти по-равному участвуют во водородных связях между каолинитовыми слоями в каолините. [E.G.]

**Resümee**—Die Kristallstruktur von Kaolinit ( $P1$ ,  $a = 5,153(1)$ ,  $b = 8,941(1)$ ,  $c = 7,403(1)$  Å,  $\alpha = 91,692(3)^\circ$ ,  $\beta = 104,860(3)^\circ$ ,  $\gamma = 89,822(3)^\circ$ , Proben von Keokuk Geoden) wurden im Detail verfeinert und die von Dickit ( $Cc$ ,  $a = 5,1460(3)$ ,  $b = 8,9376(5)$ ,  $c = 14,4244(6)$  Å,  $\beta = 96,761(5)^\circ$ ) wurden noch einmal verfeinert. Bei beiden Mineralen wurde dies anhand der Röntgenpulverdaten nach der Rietveld-Methode durchgeführt. Mit Ausnahme der Wasserstoffatome sind die Lagenstrukturen in beiden Tonen sehr ähnlich und entsprechend weitgehend den Strukturen, die bereits von anderen Autoren vorgeschlagen oder bestimmt wurden. Die Rotation in den Tetraederschichten beträgt  $7(1)^\circ$ . Die beiden inneren Hydroxyl O–H Bindungen im Kaolinit sind unterschiedlich orientiert; die eine zeigt in eine oktaedrische Lücke und die andere etwas von der Oktaederschicht weg und in Richtung des unbesetzten Zentrums eines Sauerstoffdreiecks, das durch zwei apicale Sauerstoffe und dem gemeinsamen Sauerstoff von zwei benachbarten  $SiO_4$ -Tetraedern gebildet wird. Alle sechs inneren Oberflächen-Wasserstoffatome scheinen nahezu zu gleichen Teilen an der Wasserstoffbindung zwischen den Kaolinitlagen im Kaolinit beteiligt zu sein. [U.W.]

**Résumé**—La structure cristalline de la kaolinite ( $P1$ ,  $a = 5,153(1)$ ,  $b = 8,941(1)$ ,  $c = 7,403(1)$  Å,  $\alpha = 91,692(3)^\circ$ ,  $\beta = 104,860(3)^\circ$ ,  $\gamma = 89,822(3)^\circ$ , spécimens de géodes de Keokuk) a été raffinée en détail, et celle de la dickite ( $Cc$ ,  $a = 5,1460(3)$ ,  $b = 8,9376(5)$ ,  $c = 14,4244(6)$  Å,  $\beta = 96,761(5)^\circ$ ) a été re-raffinée, toutes deux à partir de données de diffraction avec la méthode de Rietveld. A part les atomes d'hydrogène, les structures de couches dans les deux argiles sont très semblables et sont proches de ce que d'autres avaient précédemment inféré ou déterminé. La rotation dans le feuillet tétraédral est  $7(1)^\circ$ . Les deux liens intérieurs hydroxyls O–H dans la kaolinite sont orientés différemment; l'un se dirige vers un site octaédral vacant, et l'autre quelque peu dans une direction opposée à la feuille octaédrale et vers le centre inoccupé d'un triangle oxygène formé par les deux oxygènes apicaux et l'oxygène basal partagé par deux tétraèdres  $SiO_4$  adjacents. Les six atomes d'hydrogène de la surface intérieure semblent être presque également impliqués dans les liens d'hydrogène entre les couches de kaolinite dans la kaolinite. [D.J.]